Supplementary information for Physical chemistry Chemical Physics

Abnormal elastic modulus behavior in a crystalline-amorphous core-shell nanowire system

Jeong-Hwan Lee[a], Su-Ji Choi[a,b], Ji-Hwan Kwon[a], Do Van Lam[c,d], Seung-Mo Lee[c,d], An-Soon Kim[a,d], HionSuck Baik[e], Sang-Jeong Ahn[a,d], Seong-Gu Hong[a,d] ,Yong-Ju Yun[f] and Young-Heon Kim[a,d,*]

[a] Korea Research Institute of Standards and Science, 267 Gajeog-Ro, Yuseong-Gu, Daejeon 34113, Republic of Korea.

[b] Department of Materials Science and Metallurgical Engineering, Kyungpook National University, Daegu 41566, Republic of Korea.

[c] Korea Institute of Machinery and Materials, 156 Gajeongbuk-Ro, Daejeon 34103, Republic of Korea.

[d] Korea University of Science and Technology, 217 Gajeong-Ro, Yuseong-Gu, Daejeon 34113, Republic of Korea.

[e]Korea Basic Science Institute, 154 Anam-Ro, Seoul 02841, Republic of Korea.

[f]Konkuk University, 120 Neungdong-Ro, Seoul 05029, Republic of Korea.

***Corresponding authors:**

Young-Heon Kim, Tel.: +82-42-868-5449, E-mail: young.h.kim@kriss.re.kr

Supplementary information S1: Sample preparation

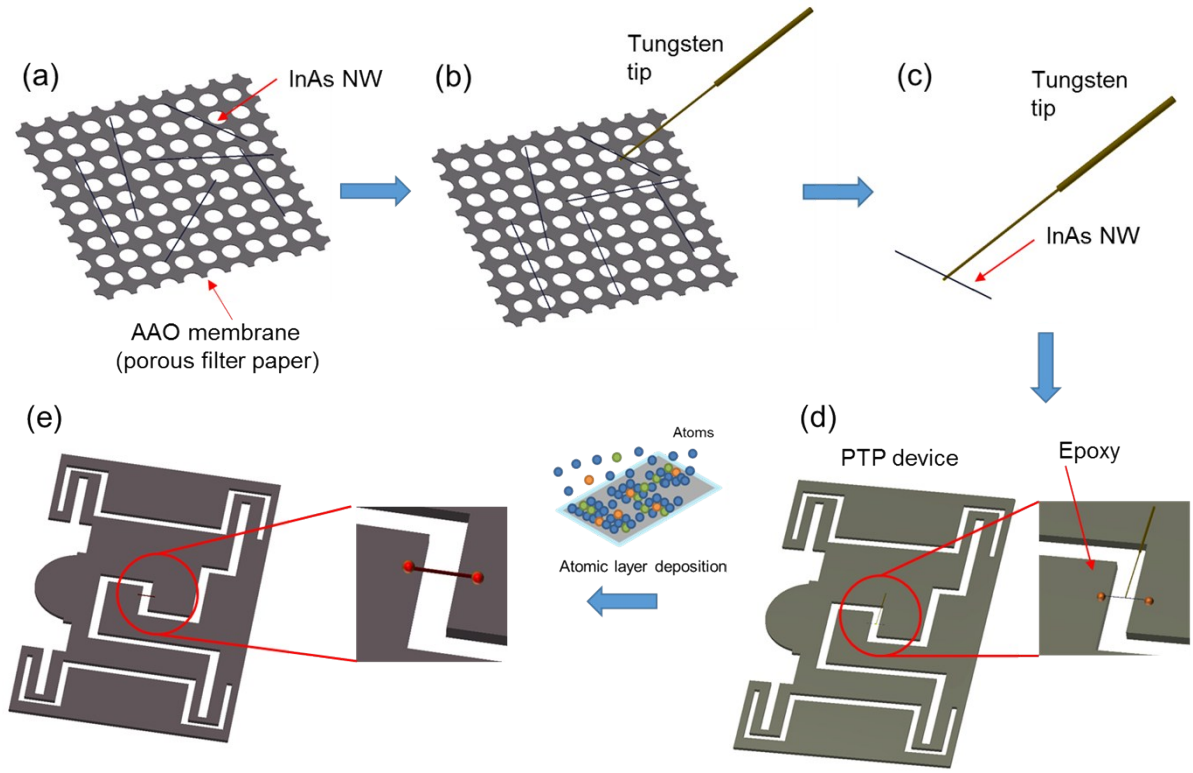

Fig. S1 Schematic illustration of the sample preparation. (a) Dispersing the InAs NWs on the AAO membrane. (b-c) Transferring a single InAs NW by using the tungsten tip. (d) Placing the InAs NW on the PTP and fixing the InAs NW with epoxy. (e) Performing atomic layer deposition.

Supplementary information S2: Atomic structure of InAs NW before and after ALD

In this study, the atomic layer deposition of Al_2O_3 was performed at a working temperature of 70 ℃, which is not high enough temperature to change the crystalline property and the phase of InAs NW [1, 2]. We proved this assumption by comparing the HR-TEM images and the selected-area electron diffraction (SAED) patterns of InAs NW and InAs/Al_2O_3 core-shell NWs. According to Fig. S2, the stacking fault on the {111} plane, represented by the strong streaks in SAED patterns, were still present in InAs/Al_2O_3 core-shell NWs. In addition, the relative positions of the diffraction spots in the inset in Fig. S2 b are same as those in the inset in Fig.S2 a, which indicates that the crystalline property of the InAs surrounded by Al_2O_3 layers, e.g. symmetry and lattice constant, is same as that of pristine InAs NW. Because the atomic and electronic structure of InAs NW did not change during the Al_2O_3 coating, the elastic modulus of InAs NW is constant regardless of the shell existence.

According to the previous studies, the interfacial oxide such as In-oxide and As-oxide were formed between InAs NW and Al_2O_3 shell during the Al_2O_3 deposition [3]. However, the thickness of those oxide layer was almost 0.8 nm, containing 0.5 nm of In-oxide and 0.3 nm of As-oxide. Although the elastic modulus of interfacial oxide (i.e., 145 GPa for In-oxide) [4] are obviously different from that of InAs (i.e., 79 GPa), the area ratio of In-oxide and As-oxide layer to the total InAs NW is less than 5%. Therefore, the formation of interfacial oxide during the Al_2O_3 coating does not play a role to change the elastic modulus of InAs NW.

(a) (b)

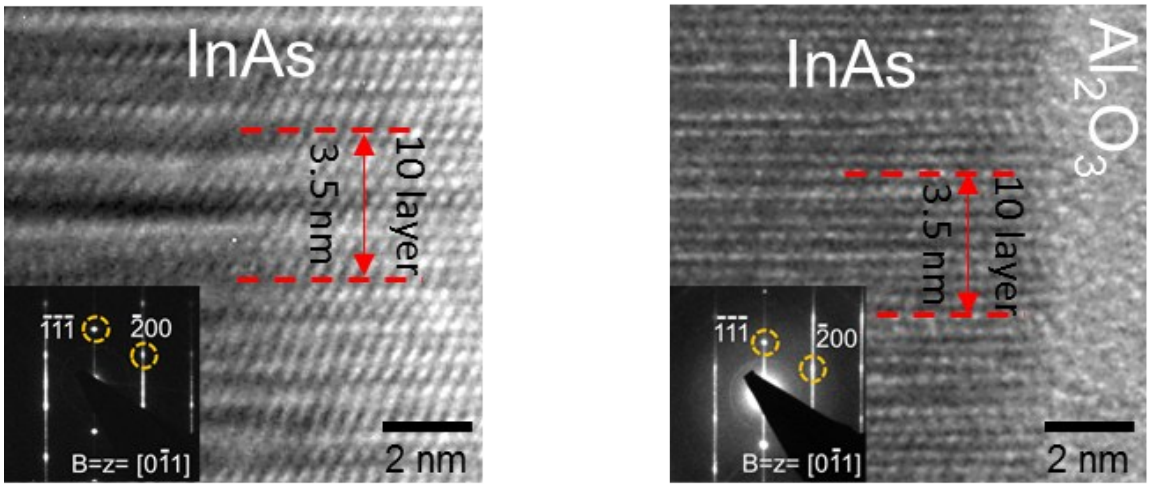

Fig. S2 HR-TEM image of (a) InAs NW and (b) InAs/amorphous Al_2O_3 (20 nm) core-shell. The stacking faults were formed along the <111> directions. The inset is the corresponding selected-area electron diffraction (SAED) pattern.

1. B. T. Meggitt, E. H. C. Parker and R. M. King, *Appl. Phys. Lett.*, 1978, **33**, 528–530.

2. C. E. C. Wood, K. Singer, T. Ohashi, L. R. Dawson and A. J. Noreika, *J. Appl. Phys.*, 1983, **54**, 2732–2737.

3. R. Timm, M. Hjort, A. Fian, B. M. Borg, C. Thelander, J. N. Andersen, L.-E. Wernersson and A. Mikkelsen, *Appl. Phys. Lett.*, 2011, **99**, 222907.

4. L. Filipovic and S. Selberherr, *Sensors*, 2015, **15**, 7206–7227.

Supplementary information S3: The comparison between E_s at the shell thickness of 20 and 40 nm

The measured E_s of 20 nm-thick shell is ~ 0.2 GPa (i.e., average) larger than that of 40 nm-thick shell. Although this gap is smaller than the corresponding value of predicted elastic modulus, obtained by Eq.2 (~ 4 GPa), the errors between measured and predicted elastic modulus at the shell thickness of 20 nm and 40 nm are 2.2 % and 1.2 %, respectively. We concluded that these error values are reasonable when considering the uncertainty of measurement. (see Fig. S3)

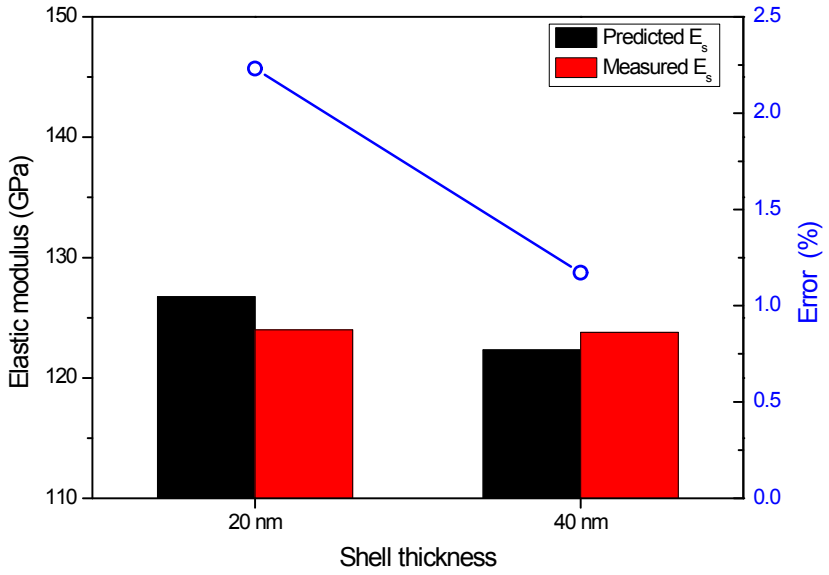

Fig. S3 The comparison of predicted E_s and experimental E_s in the shell thickness range from 20 nm to 40 nm

Supplementary information S4: BOE etching time vs. Shell thickness

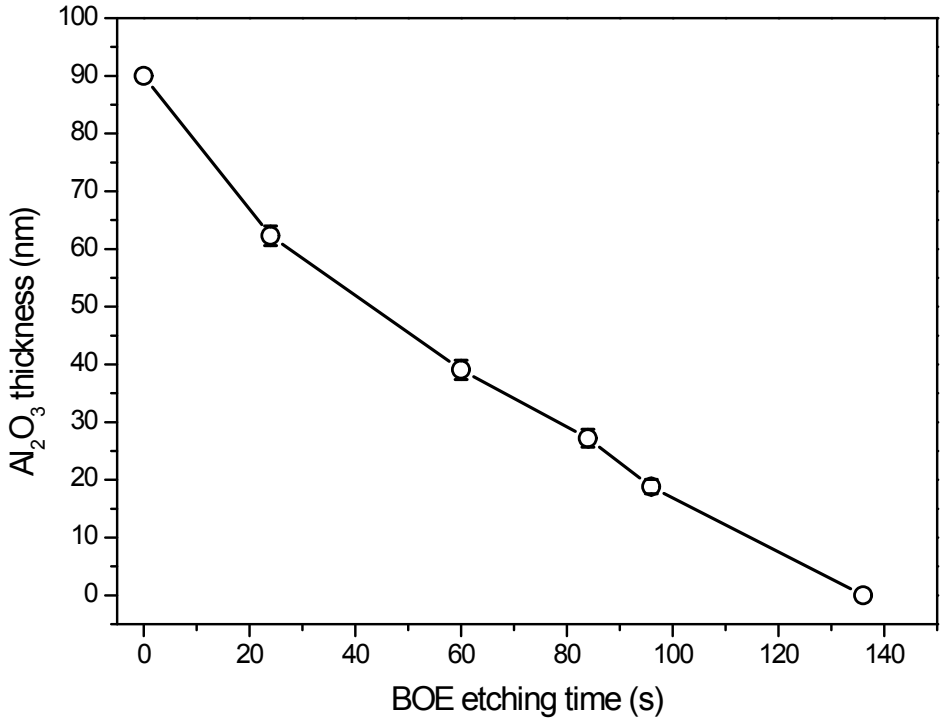

Fig. S4 (a) Thickness of the Al_2O_3 against the BOE etching time.

Supplementary information S5: Electron energy loss spectroscopy measurement in Al_2O_3 shell

In order to explain a difference of structural features between inner and outer region of the shell, we performed the electron energy loss spectroscopy (EELS) experiment. EEL spectra was obtained by using FEI Titan cube G3 80-300 S/TEM. The FEI Titan cube G3 80-300 was equipped with double Cs correctors and Gatan image filter Quantum ER (Gatan, Inc). The EELS experiment was performed at 120 keV to minimize the electron beam damage. The camera length was 115 mm, the collection angle was 14.37 mrad, and dispersion was 0.1 eV/channel. The EEL spectra were obtained from two regions in the amorphous Al_2O_3 shell where ~20 nm (inner site) and ~70 nm (outer site) from the InAs NW/a-Al_2O_3 interface, respectively. The EELS experiment was performed after the in-situ tensile test. (see Fig. S5a).

The result was shown in Fig. S5b. The overall shape of the Al 2p edge in the inner shell (~20 nm from the interface) is similar to that of α-Al_2O_3 crystalline phase [1,2], indicating that the bonding characteristics of amorphous Al_2O_3 and the α-Al_2O_3 phase are close to each other. However, the shape of Al 2p edge is significantly changed in the outer shell; the intensity of the peak at ~80 eV decreased compared to that of inner shell, the peak at ~100 eV shifts to lower energy by ~2 eV. In addition, the pre-edge shoulder was observed at ~73 eV in the outer shell, which is absent in the inner shell (the onset of the Al 2p edge is at ~75.7 eV in the inner shell). A similar pre-edge shoulder can be observed in the γ-Al_2O_3 crystalline phase [1,2], where 4-coordinated (tetrahedral) Al site exist, which indicate that the outer shell of the amorphous Al_2O_3 contains a tetrahedrally bonded Al feature. Note that the α-Al_2O_3 crystalline phase contains only 6-coordinated (octahedral) Al [1,2]. Based on the EELS data, we expect that the bonding characteristics of inner and outer shell of amorphous Al_2O_3 are similar to that of α-like Al_2O_3 and γ-like Al_2O_3 crystalline phases, respectively.

(a) (b)

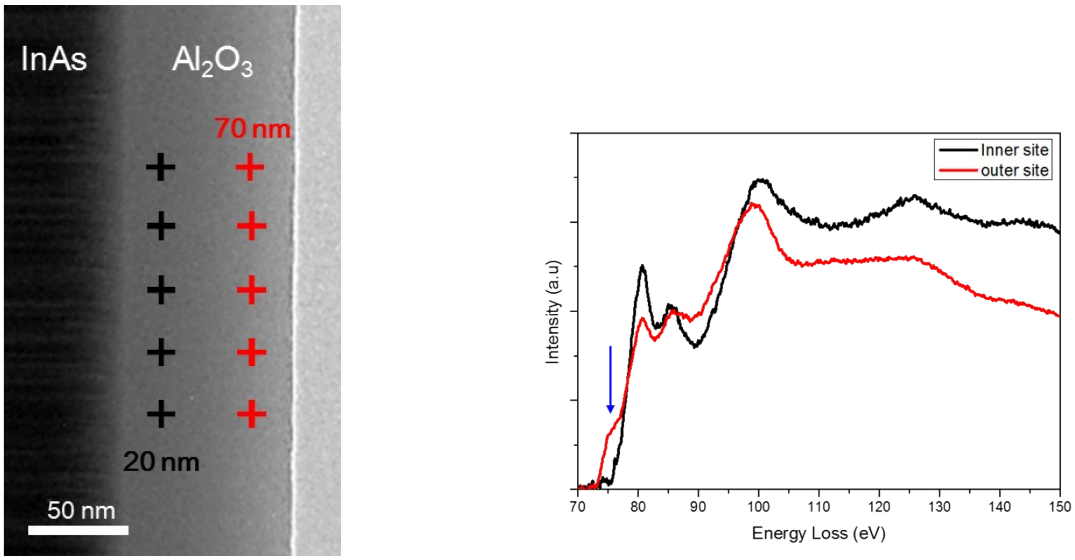

Fig. S5 (a) EELS measurement position in amorphous Al_2O_3 shell, (b) The average EELS measurements, Al $L_{2,3}$-edge, at two different thicknesses (i.e., ~20 nm - inner site and 70 nm – outer site). The spectra is background subtracted.

1. L. Bloch, Y. Kauffmann and B. Pokroy , *Cryst. Growth Des.*, 2014, **14**, 3983–3989.

2. R. Brydson, *J. Phys. D. Appl. Phys.*, 1996, **29**, 1699–1708.

Supplementary information S6: Atomic layer deposition characteristics

(a)

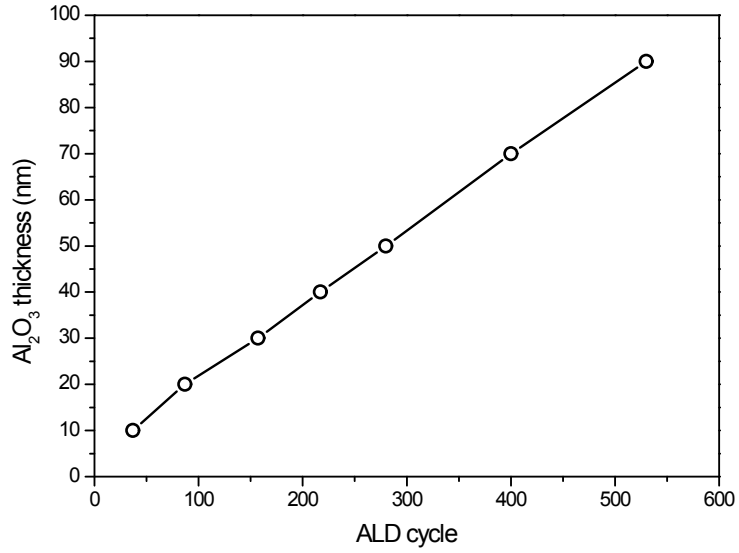

(b)

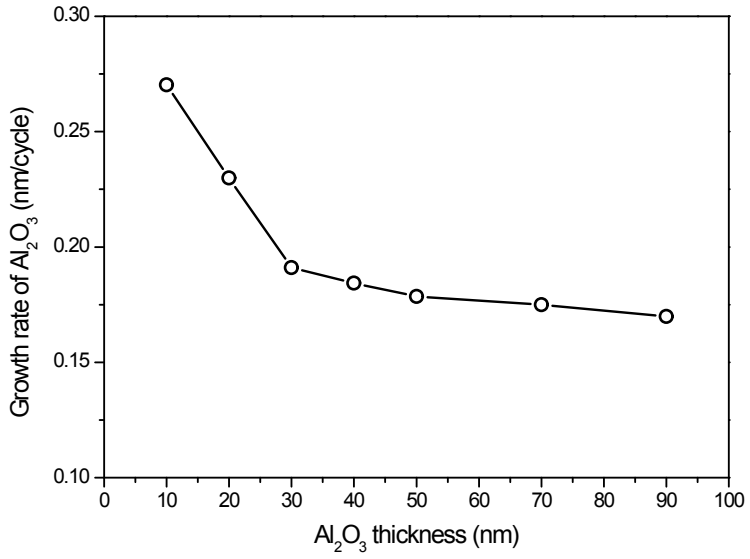

Fig. S6 (a) Thickness of the Al_2O_3 against the number of ALD cycles. (b) Growth rate of Al_2O_3 as a function of deposition thickness.